IN SITU LUBRICATION WITH BORIC ACID: POWDER DELIVERY OF AN ENVIRONMENTALLY BENIGN SOLID LUBRICANT

By

TIMOTHY PAUL BARTON

A THESIS PRESENTED TO THE GRADUATE SCHOOL
OF THE UNIVERSITY OF FLORIDA IN PARTIAL FULFILLMENT
OF THE REQUIREMENTS FOR THE DEGREE OF
MASTER OF SCIENCE

UNIVERSITY OF FLORIDA

2008

ACKNOWLEDGMENTS

First and foremost, I would like to sincerely thank my family, my grandmother, Virginia Smith, my mother, Michele Barton, my sisters Bonnie and Beth, and my girlfriend Merigan Craig, for their unending support, motivation, and understanding throughout this entire academic endeavor. It is with the love from this well of inspiration that I am able to finally complete this journey.

A very important acknowledgement goes out to my graduate advisor, Dr W. Gregory Sawyer, without whom I would have never found direction and certainly not completed my graduate thesis. His support, academic, financial, motivational, helped to inspire me to complete this degree. I would also like to acknowledge all members of my committee, both past and present. Dr. John Schuller, Dr Nam Ho Kim, Dr John Zeigert, and Dr Tony Schmitz all played a great part in my academic growth, and I sincerely appreciate all of their efforts.

I would like to thank Dr. Dan Dickrell, Pam Dickrell, and Ali Erdimer for their assistance and lending their insight with their previous works with using boric acid as a solid lubricant. I would like to note the members of the tribology lab, Dave Burris, Jason Steffans, and the rest and thank them for their help in getting acclimated to the lab, and certainly for their understanding as I made my way, often painfully for those around, through these experiments. I would also like to acknowledge anyone else who was involved with the administrative, academic, and financial efforts to complete this thesis.

TABLE OF CONTENTS

LIST OF TABLES

LIST OF FIGURES

Abstract of Thesis Presented to the Graduate School
of the University of Florida in Partial Fulfillment of the
Requirements for the Degree of Master of Science

IN SITU LUBRICATION WITH BORIC ACID: POWDER DELIVERY OF AN ENVIRONMENTALLY BENIGN SOLID LUBRICANT

By

Timothy Paul Barton

May 2008

Chair: W. Gregory Sawyer
Major: Mechanical Engineering

In-situ deposition of boric acid in dry powder form is investigated as a potential environmentally benign solid lubricant for sliding metal contacts. Boric acid is widely used in industrial processes and agriculture, is not classified as a pollutant by EPA, and produces no serious illnesses or carcinogenic effects from exposure to solutions or aerosols. In this study, boric acid powder is aerosolized and entrained in a low velocity jet of nitrogen gas which is directed at a self-mated 302 SS sliding contact in a rotating pin-on-disk tribometer. The effects of powder flow rate, sliding speed, normal load, and track diameter on coefficient of friction and wear rate are investigated. Friction coefficients below μ=0.1 can be consistently reached and maintained as long as the powder flow continues. Wear rates are reduced over 2 orders of magnitude.

CHAPTER 1
INTRODUCTION

1.2 Introduction to Petroleum Based Lubricants

Petroleum based lubricants are widely used in the manufacturing and industrial sectors, as well as in automotive and many other mass market products. It is well recognized that the use of these lubricants introduces significant quantities of used petroleum based substances into the waste stream [1]. These lubricants impose significant negative impacts to the environment and health both during their primary use and after disposal [2]. This study introduces a lubrication concept aimed at reducing the need for petroleum based fluids in a wide range of industrial processes and consumer applications by delivery of boric acid, an environmentally benign solid lubricant, in powder form. The proposed lubricant and delivery method will avoid the waste stream and environmental and health impacts associated with other lubricants used in many industrial processes and products. This technique is not tied to any particular process or product, but rather it has broad applicability; although customized delivery strategies will need to be developed for the various applications.

1.2 Environmental Concerns

The environment has long been an afterthought regarding manufacturing concerns, with the exception of clean up costs. As social awareness towards the environment rises to critical levels, the impacts of industrial waste streams on the environment is subject to increased scrutiny and requiring meaningful action. As of 1995 in the United States, 32% of all lubricants return to the environment in a physically or visually altered state [1]. Their impacts on water and air quality, wildlife, and human health have been found to be toxic. The behavior of the lubricant when returning to the environment will govern the impairment to the environment. It follows

that there is significant push to develop lubricants with reduced toxicity and increased biodegradability.

1.3 Health Concerns

Machining lubricants pose significant health hazards to human from both direct and indirect contact. Some risks of lubricants include the development of nitrosamines in coolants, skin disease from unprotected contact, carcinogens in used oils and lubricants, solvent containing products, and heavy metal compounds in additives [2]. If not properly tended to, metalworking fluid circuits can be subject to rancidity. Microorganisms such as bacteria, mold, and yeast cause rancidity by multiplying in metalworking fluid circuits once exposed to air and water dilution. Skin dermatitis has been linked to microorganism infected metalworking fluid mixtures [3]. Significant odor issues can also arise and respiratory irritation and infections have been linked to rancidity of metalworking fluids.

1.4 Cost Concerns

The increasingly stricter environmental regulations and corresponding enforcement are reducing the flexibility of metalworking fluids. As new metalworking formulations are developed, they are missing Pb, S, or Cl compounds, which provide superior machinability characteristics and are cost effective to produce. As noted above, the health and environmental concerns of the metalworking fluids are cause for increased maintenance and disposal costs. The labor and overhead costs in the U.S. in 1995 were estimated over $300 billion. These costs were estimated to comprise approximately 5-6% of the total manufacturing costs in the U.S in 1995. The costs associated with the use of cutting fluids, including purchase, maintenance, storage, and disposal, is estimated to be about 16% of the manufacturing costs, many times more than the labor and overhead costs [4].

1.5 Manufacturing Concerns

There have been many attempts to address the issue of reducing or eliminating petroleum based lubricants from metal working processes. The impact of Minimum Quantity Lubricant (MQL) volumes in machining was studied by Machado and Wallbank [5]. They compared the use of dry cutting (no lubricant), an air-water mixture, and air-soluble oil lubricant (MQL) jet streams versus overhead flood coolant in lathe cutting process. The results for cutting and feed forces, surface finish, and tool life for MQL rivaled or exceeded those of standard flood cooling at low cutting speeds. However, the effectiveness of MQL diminished as machining speeds approached those commonly used in industry. MQL lubrication also introduces a significant health risk by promoting a mist in the environment, requiring an extensive exhaust extraction system. The results for air and water lubrication were promising, however, significant corrosion problems were noted.

Kustas et al. [6] investigated the use of nanocoating on the cutting tools in a dry machining operation. The attempt of the study is to prove the coatings will generate less heat during machining and/or take away heat generated rapidly in dry machining by other means. One hundred bilayer 13Angstrom B_4C / 18 Angstrom W nanocoatings were deposited on cemented WC-Co tools and HSS drills. Coated and uncoated dry machining tests were conducted. A 33% reduction in torque requirement and a noticeable reduction of wear on the tool flank surfaces were observed. No comparison between coated tool dry machining and non coated traditional petroleum based lubricant machining was made. Significant efforts are being made to reduce or eliminate the use of traditional petroleum based lubricants. Though none has yet risen to provide the combination of surface quality, production cost, and tool life to supplant the standard lubricants.

1.6 Legal Concerns

There are currently no US laws requiring the use of eco-friendly lubricants, but two regulations, Executive Order 12873 (EO 12783) and the Great Lakes Water Quality Initiative (GLWQI), have made significant impacts on the use and disposal of conventional lubricants. EO 12783 provides preferential treatment of government contracts for bidders who use recycled oils and/or use environmentally compatible oils where possible. The Great Lakes Water Quality Initiative puts stringent requirements on zinc limitations such that the use of zinc containing lubricants is effectively banned. Government regulations on use of environmentally harmful lubricants, though placing limits on human activity with regards to the environment, are far from exhaustive and many problems exist in spite of them. Over 30% of all lubricants return to the environment in a harmfully altered state. Outside the realm of regulation, there exists a need to find an environmentally benign alternative to the current petroleum based lubricants without sacrificing manufacturing quality or dramatically increasing costs.

CHAPTER 2
LITERATURE REVIEW

2.1 Boric Acid

This experiment explores the potential of boric acid as an environmentally viable alternative to the petroleum based lubricants used today. Boric acid, whose chemical formula is H_3BO_3, is also known as orthoboric acid or boracic acid. Boric acid is a hydrate of boric oxide, B_2O_3. When boric oxide comes into contact with water, it will readily hydrate and convert to H_3BO_3. Boric acid is a weakly acidic white powder that is soluble in water, approximately 27% by weight in boiling water and 6% at room temperature. It is soft, ductile, stable, free flowing, and easily handled. Finely ground technical grade boric acid powder (>99% pure) is readily available for under $2US per pound.

2.2 Health and Environmental Impact

The Environmental Protection Agency has established that boric acid is benign and it is not classified as a pollutant under the Clean Water Act or the Hazardous Air Pollutants Act of 1990. Material safety data sheets for boric acid show no serious illness or carcinogenic effects from exposure to solutions or aerosols.

The US is the world's largest producer of boron compounds [12]. Boric acid is recovered from brines at Searles Lake in California, with large domestic reserves of boron materials residing in other lake sediments and brines. Large quantities of boron ore are also collected from an open pit mine in California.

The consumption of boric acid and boric oxide in the united states is distributed among glass making (78%), fire retardant (9%), agricultural fertilizer (4%), and industrial applications such as metal plating and finishing, paints and pigments, electroplating, and cosmetics (9%) [12]. A dilute water solution of boric acid is also commonly used as a mild antiseptic and eyewash.

The use of boric acid as a food preservative apparently dates back to the ancient Greeks. The earliest available scientific study of boric acid was conducted in 1902 and reported in Science 1904 [13]. In this study, boric acid (0.5g) was introduced into food and ingested by a group of participants with each meal. This produced occasional occurrences of "fullness in the head", nausea, and loss of appetite in a few subjects.

2.3 Boric Acid as a Solid Lubricant

In the early 1990s, the lubricity of boric acid, an overlooked but extremely available and environmentally benign lamellar solid, was demonstrated by Erdimer et al. [13-16]. Figure 2-1 shows the lamellar molecular structure of boric acid.

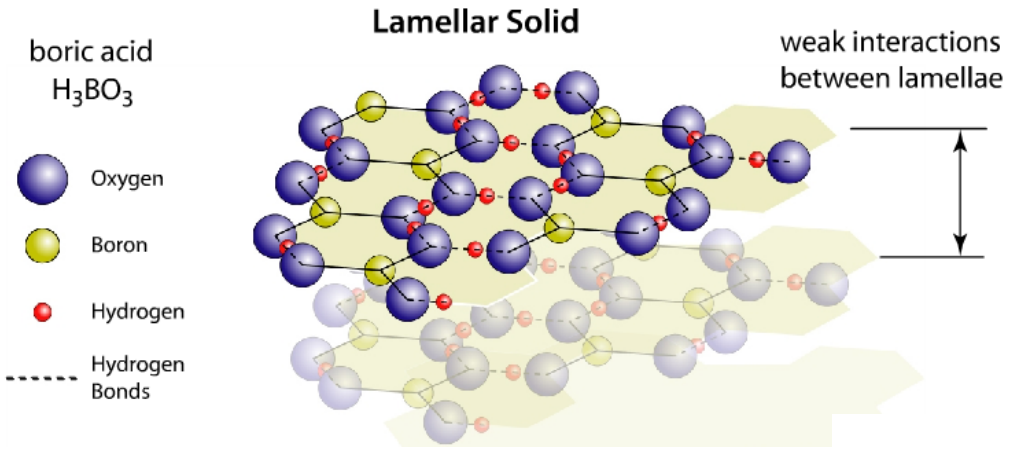

Figure 2-1. Lamellar structure of boric acid

Experiments were conducted by Gearing et al. to determine the shear strength of boric acid powder [17]. In the experiments, high pressure thrust washers were compressed against a 6111 aluminum alloy plate coated with boric acid at pressures above 500 MPa. A twisting moment was applied by the compression tool loading the washers against the plate and sheared the boric acid coating on the plate. Figure 2-2 shows the set up used in the experiment. The results determined the shear strength of boric acid to be 23 MPa.

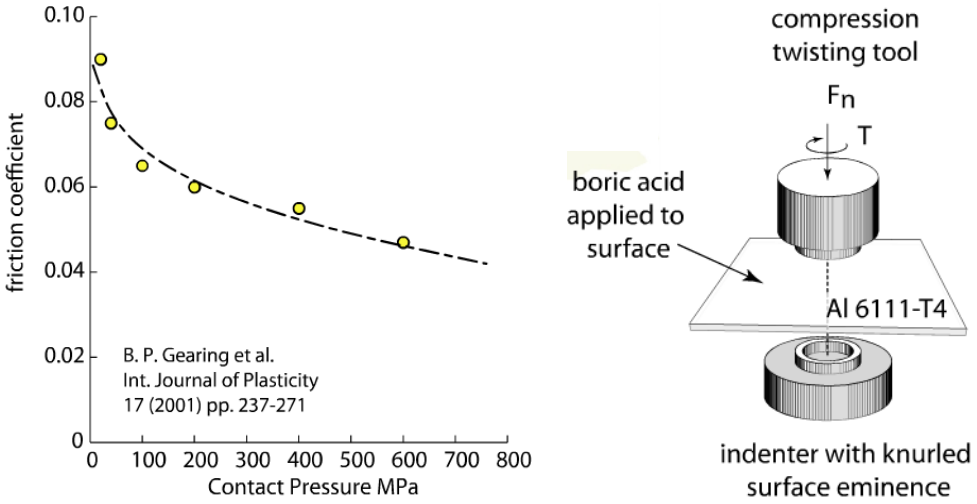

Figure 2-2. Experimental setup for Gearing et al. experiment to determine shear strength of boric acid.

The shear stress of boric acid in Gearing's study is almost the same as the experimentally determined shear stress of molybdenum disulphide, which was found to be 24 MPa by Singer et al. [18]. Figure 2-2 shows how the friction coefficient lowers with increased contact pressure and is well below 0.1 for average pressures above 100 MPa. At sub-atmospheric pressures, boric acid dehydrates and reverts back to boric oxide above 170°C. In machining applications, cutting and forming interface temperatures are expected to exceed this hydration temperature, but the contact pressures are expected to be much greater than atmospheric pressure. No published data exists, however, detailing the hydration characteristics of boric acid above 170°C at higher contact pressures.

Initial work with boric acid as a solid lubricant involved creating a solid film on the surface of the work piece. Boric acid was dissolved in either water or alcohol and the surface was coated and dried. After the solvent evaporated, the dried boric acid remained on the surface as a thin coating. This method of boric acid deposition is incompatible with many practical

applications or products in the manufacturing industry. This may be one reason that boric acid has not been accepted as a commonly used solid lubricant by industry.

Our study examined the potential of delivering dry powder via air jet to deliver sufficient lubricant to adhere to the work piece and achieve good lubrication in situ. The feasibility of boric acid powders to sustain low friction when delivered as a powder was shown by Lovell et al. [20]. In this study, a concentrated sliding contact between an aluminum pin and AISI-M50 bearing steel was loaded to an initial maximum central Hertzian contact pressure of 1.9 GPa. Figure 2-3 details the experimental setup and results.

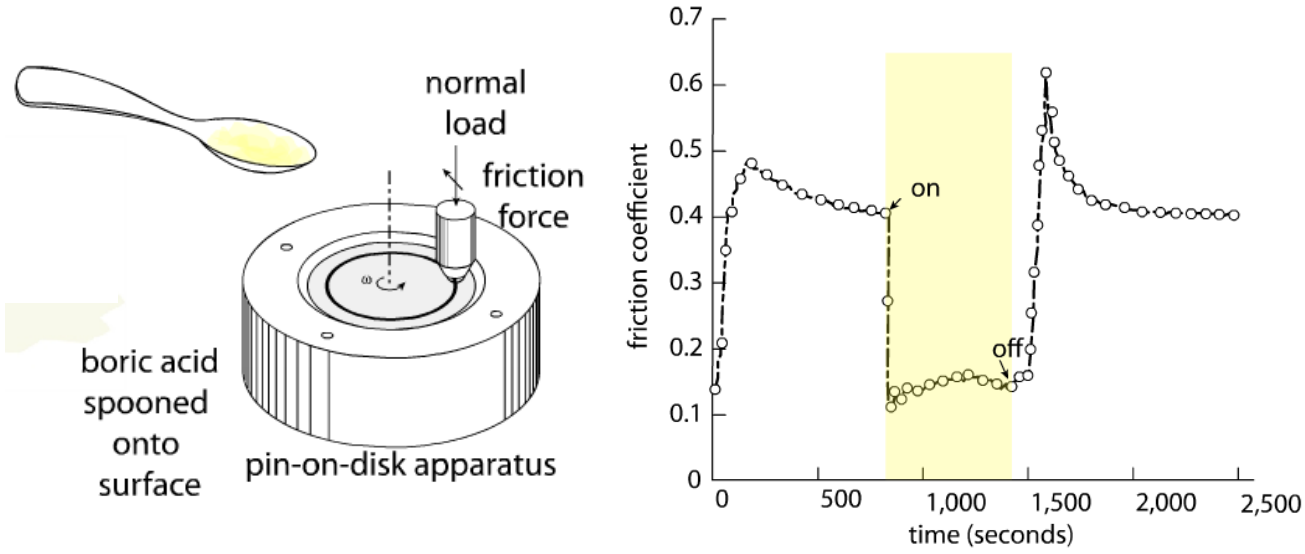

Figure 2-3. Experimental setup and results for Lovell et al. lubrication study using powder boric acid as a Solid Lubricant in a loaded pin on disk experiment

The sliding speed was approximately 1 m/s. Boric acid powder was delivered by manually sprinkling it onto the disk surface; the corresponding lubricious surface film lowered the friction coefficient from $\mu = 0.4$ to approximately $\mu = 0.15$. The friction coefficient immediately responded to the application of boric acid by dropping to low friction state. Further, the reduced friction was sustained until the powder delivery was halted.

CHAPER 3
MATHEMATICAL MODEL

We developed a predictive mathematical model for the effects of boric acid delivery on the sliding contact between the stainless steel surfaces. Assume a rotating disk has a contact interface with a stationary sphere supporting a load. If boric acid is delivered into the interface, a fraction of the powder may stick to the disk face along the wear track. The amount of boric acid on the face may be represented by a fraction of surface covered with the powder. Initial fractional coverage is represented by θ_0, where

$$\theta_0 = \frac{A_{H_3BO_3}}{A_{total}} \tag{3-1}$$

As powder is continuously delivered, more will be deposited on the area. An amount of the deposited powder, however, will adhere over top already covered surface. The coverage after a platelet of material $\Delta\theta$ has been deposited on a surface with fraction coverage given by Equation 3-1 is

$$\theta_{0+1} = \theta_0 + \Delta\theta - \Delta\theta \cdot \theta_0 \tag{3-2}$$

This pattern of application of boric acid platelets continues during powder exposure for n platelets

$$\begin{aligned}
\theta &= \theta_0 \\
\theta_1 &= \theta_0 + \Delta\theta - \Delta\theta \cdot \theta_0 \\
\theta_2 &= \theta_0 + 2 \cdot \Delta\theta - 2 \cdot \Delta\theta \cdot \theta_0 - \Delta\theta^2 + \Delta\theta^2\theta_0 \\
\theta_3 &= \theta_0 + 3 \cdot \Delta\theta - 3 \cdot \Delta\theta \cdot \theta_0 - 3 \cdot \Delta\theta^2 + 3\Delta\theta^2\theta_0 + \Delta\theta^3 - \Delta\theta^3 \cdot \theta_0
\end{aligned} \tag{3-3}$$

After reorganization the above pattern, namely by factoring out the $\Delta\theta$ terms, the sequence of Equation 3-3 can be equivalently expressed as

$$\theta = \theta_0$$
$$\theta_1 = \theta_0 + \Delta\theta \cdot (1 - \cdot\theta_0)$$
$$\theta_2 = \theta_0 + 2 \cdot \Delta\theta \cdot (1 - \theta_0) - \Delta\theta^2 \cdot (1 - \theta_0) \quad (3\text{-}4)$$
$$\theta_3 = \theta_0 + 3 \cdot \Delta\theta \cdot (1 - \theta_0) - 3 \cdot \Delta\theta^2 \cdot (1 - \theta_0) + \Delta\theta^3 \cdot (1 - \theta_0)$$

This pattern can be equivalently expressed by the following series expression

$$\theta = \left(\sum_{a=0}^{n} \frac{n! \cdot \Delta\theta^a \cdot (1 - \Delta\theta) \cdot (-1)^{(a+1)}}{a! \cdot (n-a)!} \right) + 1 \quad (3\text{-}5)$$

Equation 3-5 can then be expressed in the compact and closed form

$$\theta = 1 - (1 - \theta_0) \cdot (1 - \Delta\theta)^n \quad (3\text{-}6)$$

Equation 3-6 assumes that n platelets of boric acid powder sprayed into the interface stick to the surface during a single revolution of the disk. After contact with the pin a fraction of the material is removed. λ is now introduced as a loss term indicating the amount of powder removed each cycle by contact pressure between the pin and disk. Loss factor, λ, is assumed to be a linear coefficient term between 0 and 1 relating the coverage fraction of the disk surface covered by the pin leaving of the contact interface to the coverage fraction of the disk surface entering the contact interface. Factors affecting λ include the normal load applied to the surface through the pin as well. The terms of this relationship are defined below

θ_{in} = Coverage fraction entering contact interface
θ_{out} = Coverage fraction exiting contact interface
λ = Loss Factor

The coverage fraction leaving the contact interface is then defined as

$$\theta_{out} = \lambda \cdot \theta_{in} \quad (3\text{-}7)$$

Substituting Equation 3-6 into Equation 3-7 yields the following expression to determine the fractional coverage for any given rotation N. This captures the transient behavior of the coupled film deposition and removal process.

$$\theta_{i,N} = 1 - (1 - \lambda \cdot \theta_{i,N-1}) \cdot (1 - \Delta\theta)^n \tag{3-8}$$

Where N is the current cycle and n is the number of platelets that are deposited each revolution of the disk. The final solution to the coupled deposition and removal sequence is

$$\theta = \frac{\lambda^N \cdot ((1-\Delta\theta)^n)^N - \lambda^N \cdot ((1-\Delta\theta)^n)^{(N+1)} - 1 + (1-\Delta\theta)^n}{\lambda \cdot ((1-\Delta\theta)^n)^N - 1} \tag{3-9}$$

The exponent n is the number of platelets deposited on any fractional area of the surface between contacts. Powder mass flow rate is assumed to have a directly proportional effect on n, as higher flow would increase the coverage fraction per unit time. Surface speed of the pin on the disk is assumed to have an inversely proportional impact on n, as a faster surface speed would reduce the amount of time for powder to enter the contact interface. Given these considerations, the exponent n is assumed to be predicted by the following expression

$$n \propto \frac{\dot{m}}{\omega \cdot r} \tag{3-10}$$

where $\dot{m}$ = mass flow rate (g/sec)
ω = spindle speed (rad/sec)
r = radial pin location (mm)

The term N is the cycle count and can be calculated by

$$N \propto \frac{\omega \cdot t}{2\pi} \tag{3-11}$$

where $t =$ time (sec). The term λ describes the powder removal through the pin on disk interface as a ratio of coverage fraction exiting the interface to the coverage fraction entering it. Greater contact pressure would displace more powder per revolution thus reducing λ. Contact pressure is determined by the normal load, F_n. It is assumed in this model that λ is logarithmically proportional to the applied normal load and is described below

$$\lambda \propto e^{(-\beta \cdot F_n)} \tag{3-12}$$

As the system approaches steady state, N approaches infinity. Equation 3-9 predicts that the λ^N term, with λ being a fraction between zero and one, will reduce to zero at steady state.

$$\theta = \frac{(1-\Delta\theta)^n - 1}{\lambda \cdot (1-\Delta\theta)^n - 1} \tag{3-13}$$

This model assumes the amount of frictional load is determined by the coverage fraction. The total friction coefficient is predicted to equal the sum of the coverage fraction for each surface condition (i.e., powder or steel) multiplied by the friction coefficient for each surface versus the pin.

$$\mu_{total} = \theta \cdot \mu_{H_3BO_3} + (1-\theta) \cdot \mu_{steel} \tag{3-14}$$

where μ_{H3BO3} is the friction coefficient between boric acid and pin material. Experimentally, Equation 3-14 will be verified by setting up an experimental matrix that varies the four parameters predicted to affect the coverage fraction. Those four parameters are normal load, spindle speed, powder mass flow rate, and radial location of the pin on disk contact interface.

CHAPTER 4
EXPERIMENTAL SETUP

For the effectiveness of the lubricating properties of boric acid powder to be characterized, experiments studying surface to surface contact, especially the friction and wear between the surfaces, needed to be conducted. The following chapter depicts the variables and methods chosen to conduct the study of boric acid as a solid lubricant in metal on metal sliding contact.

4.1 Specimen Characterization and Preparation

The Tribology Lab at the University of Florida has a pin on disk tribometer that creates relative rotating motion of a flat disk surface that maintains contact with a loaded stationary pin surface. The pin samples in this experiment were 302 stainless steel balls of 4.76 mm (0.1875") diameter purchased from McMaster Carr (part number 9291K18). As received, they had a reflective surface finish so no further processing of the ball surface was performed prior to experiment. The surface of the ball was analyzed using the Wyco Scanning White Light Interferometer at MAIC (Major Analytical Instrumentation Center) at the University of Florida. The mean surface roughness of the balls was 150 nm. The rotating surfaces in the experiment were from 302 stainless steel disks with a 50.4mm (2.0") diameter. The disks were manufactured from round stock purchased from McMaster Carr. The round stock was cut into 0.250 in. disks on a machine shop band saw. The disk surfaces were prepped using 3 stages of sanding and polishing, using 100 grit, 250 grit, and 600 grit polishing paper, until all manufacturing marks were removed and a mirror finish was obtained. Surface roughness measurements on the prepared disk surface were repeated on 15 samples using white light interferometry. Table 4-1 displays the results of these surface measurements. Average surface roughness of the disks was calculated to be R_a 172 nm, □ = 3 nm. Prior to installation to the apparatus, each sample, pin and disk, were washed and sonicated in methyl alcohol.

Table 4-1. Surface Roughness Measurement results for prepared surface of 302 Stainless Steel disks. Measurements performed on the WYCO White Light Interferometer at the Major Instrumentation Analytical Center (MAIC) at the University of Florida

Scan #	R_a (nm)	R_{ms} (nm)	20 Point Peak to Valley (mm)	2 Point Peak to Valley (mm)
1	288.0	367.1	3.3	3.8
2	287.5	366.2	3.3	3.8
3	287.5	366.0	3.4	3.9
4	286.4	364.8	3.3	3.7
5	286.4	364.7	3.3	3.6
6	288.2	367.1	3.3	3.7
7	287.8	366.5	3.3	3.6
8	287.6	366.2	3.2	3.8
9	287.7	366.3	3.2	3.6
10	287.5	366.1	3.3	3.9
11	288.0	366.7	3.4	4.3
12	286.3	364.7	3.3	3.7
13	287.2	365.8	3.3	3.7
14	287.5	366.3	3.3	3.7
15	289.2	367.9	3.3	3.6
Ra Avg	*Ra Std Dev*			
287.5	**0.7**			

The powder used in this study was technical grade (99% pure) with particle sizes ranging from a few micrometers up to 100+ micrometers. The boric acid was purchased from Fischer Chemical, p/n A74-3. The particle size of the powder was measured under an SEM at Major Analytical Instrumentation Center at UF. Figure 4.1 shows the SEM photos of the boric acid. Figures 4-2 and 4-3 show the diagram of the Pin On Disk system and apparatus used in this experiment.

4.2 Pin on Disk Tribometer

The pin on disk tribometer used in this experiment is shown in Figure 4-3 . Measurements from the pin on disk tribometer were made through a compression load cell.

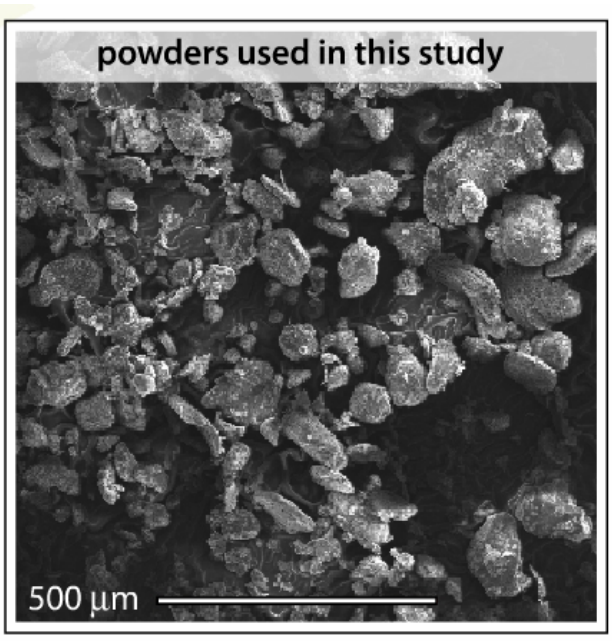

Figure 4-1. Actual boric acid powder used in this experiment taken using the Scanning Electron Microscope at the University of Florida

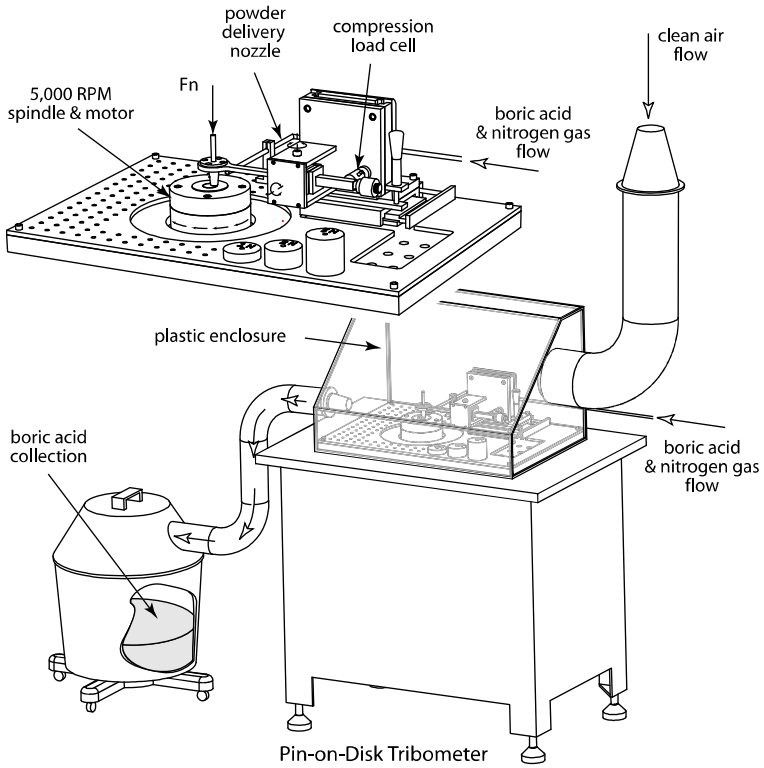

Figure 4-2. Rotating pin-on-disk tribometer used in this study. Airborne particle management handled with the shop vacuum and filter stack.

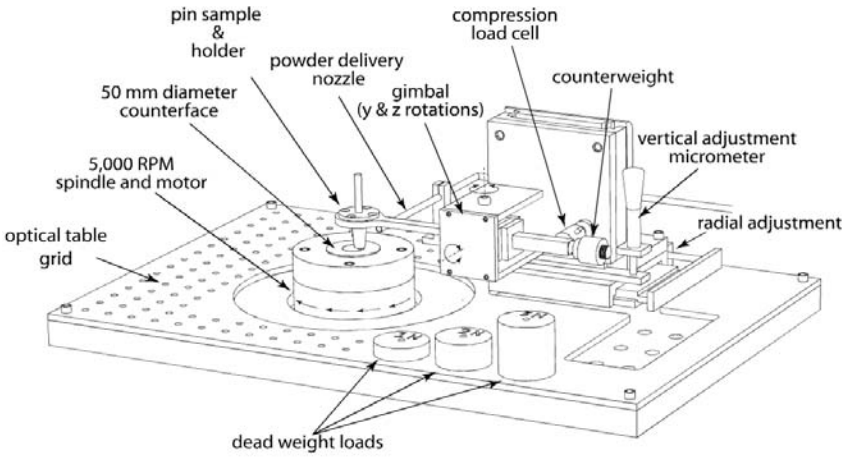

Figure 4-3. Rotating pin-on-disk tribometer used in this study.

The load cell measured force from the pin sample holding arm due to the frictional loading of the pin from the rotating disk. The other end of the arm supported the static load and fixed the stationary ball to the desired location on the disk surface. Disk samples were fixtured to the spindle and the testing surface exposed to contact with the pin sample. The pin on disk tribometer spindle and motor had the capacity to rotate up to 4700 rpm in either clockwise or counter clockwise orientation. Clockwise rotation was chosen to ensure constant contact between the sample holding arm and load cell. The arm pivoted on a gimble and was allowed pitch and yaw rotations. A threaded dead weight located at the end of the arm and a vertical adjustment micrometer allowed for adjustment to balance the pitch of the sample holding arm. When the pitch was properly balanced, the arm was considered level and an unloaded pin barely made contact with the disk surface. A radial adjustment micrometer adjusted the radial location of the system. When the system was radially balanced, the pin sat directly on the center of the disk. Radial balance was calibrated by running a pin against a disk and the radial micrometer adjusted until the wear track became a single dot.

4.3 Powder Delivery System

A system needed to be developed to aerosolize and continually deliver boric acid into the contact interface. Nitrogen gas was first compressed and cleaned through the filter stack. There it underwent two stages of filtration and desiccation to ensure gaseous purity. The nitrogen gas was then regulated to 40 PSI and again desiccated. The nitrogen passed through a flow meter, which allowed for variable flow output measured by a floating ball and calibrated scale. This flow setting was the regulation for controlling the mass flow rate of boric acid in the pin – disk interface. Out of the flow meter, the clean, dry, metered gas then passed through ¼" stainless steel pipe into the boric acid bottle, shown in Figure 4-4 below.

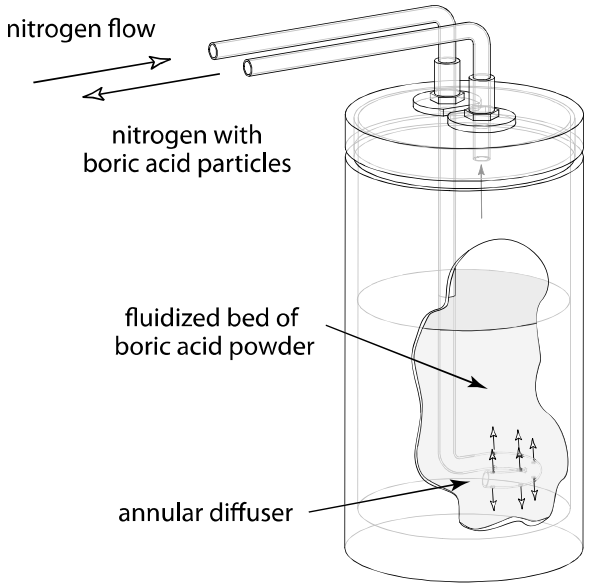

Figure 4-4**.** Particle delivery scheme. The container was mounted on a mechanical shaker during operation. Dry nitrogen gas flowrates were controlled through a series of flowmeters.

The boric acid bottle was mounted on a shaker, which allowed for enough particle agitation to fluidize the powder and minimize powder clumping. As an additional method to eliminate clumping, the powder was triple sifted prior to loading the bottle. As shown in the

figure above, the nitrogen input stem had many holes drilled through it and was formed into an annular profile to have a large contact area with the powder. When the bottle was assembled, the input stem descended into the powder. The gas pressure created a fluidized bed, which entrained boric acid particles in the output stream. From the boric acid bottle, the nitrogen–boric acid mixture flowed through a ¼" stainless steel pipe to the pin on disk interface.

The flow meter setting was calibrated for powder flow rate prior to conducting the experiments. The control variable to set the powder delivery rate was the flow meter setting, which determined the gas flow into the powder delivery system. The flow meter had convenient flow setting demarcations of 10, 20, 30, and 40. The powder container was loaded with enough boric acid to establish a system weight of 600 grams prior to each calibration run. The mass of the bottle loaded with powder was weighed prior to running gas through the system and incrementally in five minute time steps. The time steps were chosen to verify consistency of the flow rate over the run times observed throughout the experiment.

Figures 4-5 and 4-6 show the results of the powder delivery calibration. Figure 4-5 shows the total powder delivery rate where the bottle weight measurements are referenced to the initial weight and time (m_0 = 600 grams ; t_0 = 0 min). The equation defining the powder mass delivery rate referenced to t_0 and m_0 is

$$\dot{m} = \frac{m_i - m_0}{t_i - t_o} \tag{4-1}$$

where t_i is the time at iteration i and m_i is the powder mass in the bottle at time = t_i. Figure 4-6 shows the powder delivery results incrementally. Each powder delivery rate measurement referenced the previous time step. The equation defining this incremental powder mass delivery rate, which shows the impact of time on delivery rate, is given in Equation 4-2.

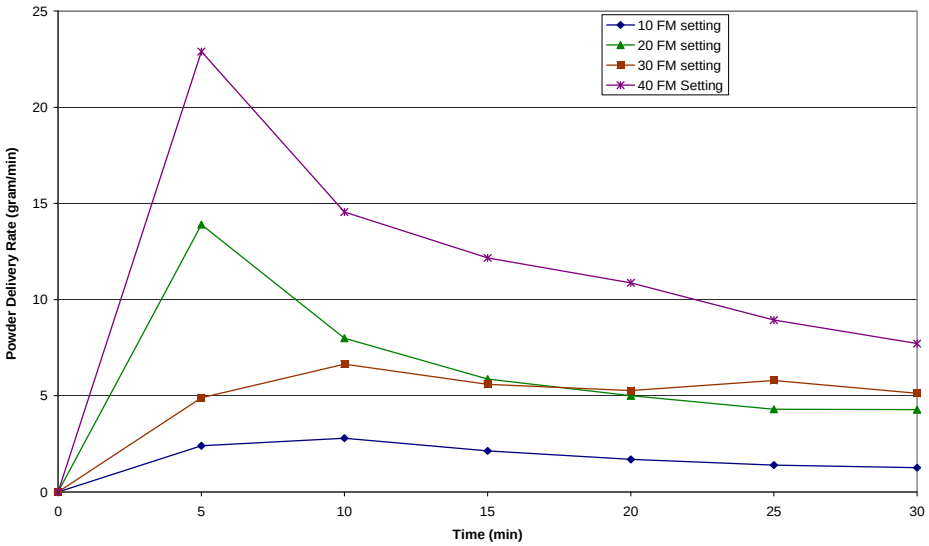

Figure 4-5. Powder delivery calibration curves referenced from initial conditions, t = 0 min; mass of boric acid in container = 600g, powder deliver rate = $(m_x - m_0) / (t_x - t_0)$

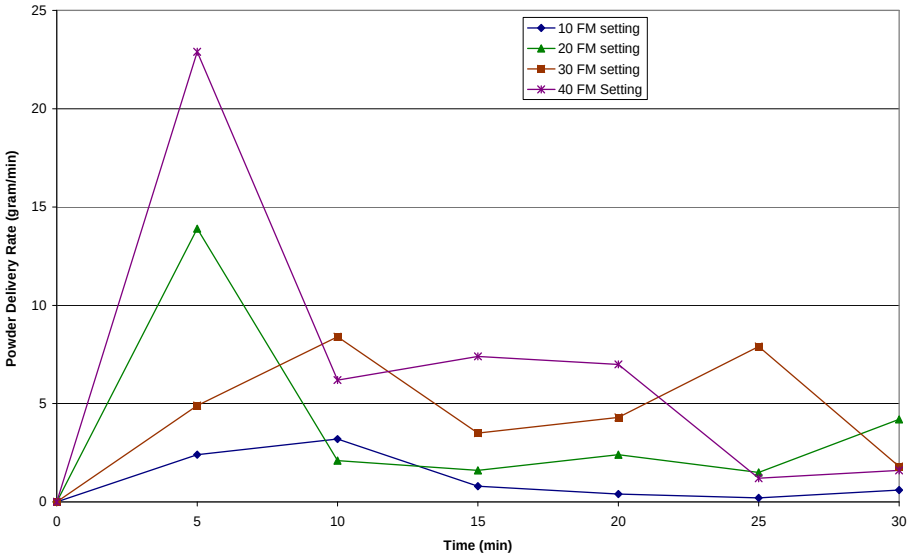

Figure 4-6. Incremental powder delivery calibration curves referenced from previous time step; powder deliver rate = $(m_x - m_{x-1}) / (t_x - t_{x-1})$

$$\dot{m} = \frac{m_i - m_{i-1}}{t_i - t_{i-1}} \tag{4-2}$$

Figures 4-5 and 4-6 show the non-linear nature of the powder delivery system. This variability is due to several factors. The most significant issue is that there is no compensation for the constant gas flow rate yet depleting powder levels. As time progressed, lesser amounts of boric acid were able to get entrained in the outflow stream. Though the powder delivery rate was not constant, the flow meter setting did correspond with a higher powder delivery rate throughout the experiment. The actual powder delivery rate was verified for each experimental run, by weighing the bottle prior to and following each run. For the experiments, settings 10, 20, and 30 were chosen. A flow meter setting of 40 for the 60 minute test runs would have required a larger powder container.

4.4 Environment Chamber

An environment chamber was implemented to the pin on disk tribometer set up to contain boric acid, which could be a slip and inhalation hazard. The panels of the environment chamber are made of Lexan sheets, providing clear view of the experimental apparatus, yet provide a lightweight assembly and removal. A 2 horsepower shop-vac pulled a vacuum to create flow throughout the chamber and reduce powder build up on the hardware. An air-filter stack was attached to the chamber opposite the shop-vac interface, with a sheet filter attached to the inlet. This provided clean air flow across the pin–disk interface.

4.5 Determination of Experimental Matrix

A matrix of testing variables was created to test the effectiveness of a continuous stream of solid boric acid into the contact surface between the pin and disk. Using the predictions of the mathematical model, the control variables were selected. The experimental parameters studied in the experiment were normal force, sliding speed, wear track diameter, and powder flow rate.

The normal force was modified by adding a dead weight to the arm directly above the pin. Sliding speed was adjusted by changing the spindle rotational speed. The adjustment for the wear track diameter was set with the radial adjustment micrometer. The powder flow rate measurement and adjustment was described in the previous section. Table 4-2 summarizes the conditions tested in the experiment.

Table 4-2. The experimental matrix (3*3*3*3) plus nine repeats at the midpoint and one unlubricated control.

Fn (N)	Ω (RPM)	Track Diameter, D (mm)	Flow Meter Setting
0.65	400	3.8	10
3.30	2,000	25.0	20
6.30	4,000	38.0	30

The experimental matrix resulted in 81 individual tests. The midpoint condition (3.3 N Load, 2000 rpm, 25.4 mm track diameter, flow meter setting = 20) was tested 9 additional times to exhibit repeatability of the friction measurement. One midpoint test with no boric acid delivery was conducted to provide a baseline measurement for friction between bare metal on metal contact. The lengths of the tests were set to maintain 24,000 rotations of the disk, where 24,000 disk revolutions were divided by the spindle speed. The combination of wear track diameter and spindle speeds allow for a range of sliding speeds that varied by 100 times.

The sequence of experiments was randomized to prevent any time-related bias as shown in Table 4-3. As described earlier, the data acquisition system collected loading measurements of the gimble arm on the load cell, which correlated to friction loads and friction coefficient of the ball on the disk. The selection of test conditions allows for significant flexibility in grouping data for analysis. For example, 27 tests were performed at constant diameter while varying sliding speed, contact force, Fn, and flow rate, f; and 18 tests were performed at constant sliding speed while varying track diameter, D, and rotational speed, Ω, Fn, and f. The variability of testing conditions allowed for an expansive, yet detailed, study of the parameters impacting the

effectiveness of a solid boric acid lubricant on the wear rates and frictional forces in pin on disk contact. Laboratory ambient conditions were measured daily before testing. Relative humidity varied from approximately 20 to 55%. The ambient temperatures ranged from 25°C to 28°C.

Table 4-3. Randomized experimental testing sequence with all parameters per run.

Run Number	Flow Meter Setting	Spindle Speed (RPM)	Dia (in)	Normal Load (grams)	Length (sec)	Run Number	Flow Meter Setting	Spindle Speed (RPM)	Dia (in)	Normal Load (grams)	Length (sec)
1	10	400	1.50	66.3	3600	46	20	2000	1.00	642.5	720
2	20	400	0.15	336.6	3600	47	30	4000	1.50	336.6	360
3	20	400	1.00	66.3	3600	48	20	2000	1.00	336.6	720
4	20	4000	0.15	66.3	360	49	10	4000	1.00	66.3	360
5	10	4000	1.50	336.6	360	50	20	400	1.50	336.6	3600
6	10	4000	1.00	642.5	360	51	20	2000	1.50	336.6	720
7	10	4000	0.15	642.5	360	52	30	400	1.50	66.3	3600
8	10	4000	1.50	66.3	360	53	10	400	1.00	66.3	3600
9	10	2000	1.50	642.5	720	54	30	4000	1.00	336.6	360
10	20	2000	1.00	336.6	720	55	30	2000	0.15	336.6	720
11	20	2000	1.00	66.3	720	56	30	4000	0.15	642.5	360
12	20	400	1.50	642.5	3600	57	20	2000	1.00	336.6	720
13	30	400	1.00	336.6	3600	58	30	400	0.15	336.6	3600
14	10	2000	0.15	642.5	720	59	30	400	1.00	66.3	3600
15	20	4000	1.00	66.3	360	60	10	2000	0.15	66.3	720
16	30	400	1.50	336.6	3600	61	10	400	0.15	66.3	3600
17	20	2000	1.50	642.5	720	62	20	4000	1.50	642.5	360
18	30	2000	0.15	642.5	720	63	30	4000	1.00	642.5	360
19	30	2000	1.50	642.5	720	64	30	400	0.15	66.3	3600
20	20	4000	0.15	336.6	360	65	20	4000	1.00	642.5	360
21	30	2000	1.00	642.5	720	66	20	4000	1.50	66.3	360
22	10	400	1.50	336.6	3600	67	30	400	1.50	642.5	3600
23	20	2000	0.15	66.3	720	68	20	2000	1.00	336.6	720
24	20	4000	1.50	336.6	360	69	30	4000	1.00	66.3	360
25	20	2000	1.00	336.6	720	70	20	400	1.00	336.6	3600
26	30	4000	1.50	66.3	360	71	30	2000	0.15	66.3	720
27	20	4000	1.00	336.6	360	72	20	400	0.15	642.5	3600
28	20	2000	1.50	66.3	720	73	20	2000	1.00	336.6	720
29	30	400	0.15	642.5	3600	74	10	2000	0.15	336.6	720
30	30	2000	1.50	66.3	720	75	20	4000	0.15	642.5	360
31	30	400	1.00	642.5	3600	76	10	4000	0.15	336.6	360
32	10	400	0.15	336.6	3600	77	10	2000	1.00	66.3	720
33	10	400	1.00	336.6	3600	78	30	4000	0.15	66.3	360
34	10	4000	1.50	642.5	360	79	10	400	1.00	642.5	3600
35	20	2000	1.00	336.6	720	80	20	2000	0.15	336.6	720
36	30	4000	1.50	642.5	360	81	20	2000	0.15	642.5	720
37	10	4000	0.15	66.3	360	82	10	2000	1.00	642.5	720
38	20	400	1.00	642.5	3600	83	20	400	0.15	66.3	3600
39	30	2000	1.00	336.6	720	84	20	400	1.50	66.3	3600
40	30	4000	0.15	336.6	360	85	10	2000	1.50	336.6	720
41	10	400	0.15	642.5	3600	86	10	2000	1.00	336.6	720
42	30	2000	1.00	66.3	720	87	20	2000	1.00	336.6	720
43	30	2000	1.50	336.6	720	88	10	4000	1.00	336.6	360
44	10	2000	1.50	66.3	720	89	20	2000	1.00	336.6	720
45	10	400	1.50	642.5	3600	90	20	2000	1.00	336.6	720

** shaded entries denote a midpoint run*

CHAPTER 5
RESULTS

The critical measurements taken in this study were the thickness of the wear track left on the sample disk and the load on the load cell. The wear track diameter and thickness are the key measurements to correlating the wear rate and ultimately the effectiveness of the boric acid powder as a solid lubricant. To measure the thickness of the wear track, an optical microscope was used. A calibrated measurement grid was attached to the scope, and the inside of the wear track was located at 0.000". The measurement at the outside of the wear track then established the wear track thickness. Measurements were made at each quadrant of the wear track to establish consistency. Those measurements were averaged and the standard deviation taken. The wear rate for the pin was used as the metric for wear in this study. To calculate the wear on the pin, the volume of material lost was first determined. Equation 5-1 was used to determine the pin volume lost due to wear. Figure 5-1 graphically shows the relationship between the wear scar diameter and the lost volume.

$$V = \frac{\pi * h^2 * (3R - h)}{3} \tag{5-1}$$

where V is the volume of the pin lost due to wear, R is the radius of the pin and h is the radial height of the lost volume. Calculated wear rates for all runs are summarized in the table below.

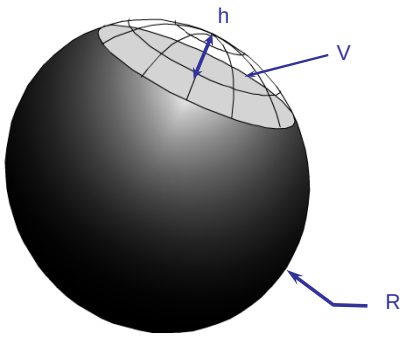

Figure 5-1 Pin volume lost due to wear during the experiment

Table 5-1. Results from the experimental matrix. **D** is wear track diameter in millimeters, **f** is commanded boric acid flowrate in grams/minute, **K** is wear-rate x 10^{-6} $mm^3/(Nm)$.

Ω = 400 RPM				Ω = 2,000RPM				Ω = 4000 RPM			
Fn = 0.65 N				Fn = 0.65 N				Fn = 0.65 N			
D	F	μ	K	D	F	μ	K	D	F	μ	K
3.8	10	0.196	2.92	3.8	10	0.157	-	3.8	10	0.090	-
3.8	20	0.080	-	3.8	20	0.094	14.93	3.8	20	0.085	-
3.8	30	0.138	-	3.8	30	0.085	1.98	3.8	30	0.092	0.63
25.0	10	0.147	0.30	25.0	10	0.036	36.65	25.0	10	0.086	0.22
25.0	20	0.122	-	25.0	20	0.035	42.48	25.0	20	0.075	-
25.0	30	0.159	0.67	25.0	30	0.062	21.31	25.0	30	0.047	4.90
38.0	10	0.147	0.44	38.0	10	0.058	1.25	38.0	10	0.080	0.21
38.0	20	0.138	0.03	38.0	20	0.077	0.38	38.0	20	0.049	4.13
38.0	30	0.173	0.19	38.0	30	0.045	1.56	38.0	30	0.089	0.57
Fn = 3.3 N				Fn = 3.3 N				Fn = 3.3 N			
D	F	μ	K	D	F	μ	K	D	F	μ	K
3.8	10	0.143	0.23	3.8	10	0.148	0.82	3.8	10	0.081	1.48
3.8	20	0.139	4.03	3.8	20	0.12	-	3.8	20	0.088	5.55
3.8	30	0.162	0.31	3.8	30	0.11	0.12	3.8	30	0.087	0.03
25.0	10	0.152	0.76	25.0	10	0.056	0.80	25.0	10	0.055	1.05
25.0	20	0.156	0.48	25.0	20	0.044*	1.54*	25.0	20	0.035	0.52
25.0	30	0.163	0.41	25.0	30	0.05	2.00	25.0	30	0.030	1.55
38.0	10	0.113	9.02	38.0	10	0.049	0.14	38.0	10	0.321	0.03
38.0	20	0.116	1.36	38.0	20	0.039	0.27	38.0	20	0.040	0.34
38.0	30	0.101	13.26	38.0	30	0.045	0.19	38.0	30	0.026	0.69
Fn = 6.3 N				Fn = 6.3 N				Fn = 6.3 N			
D	F	μ	K	D	F	μ	K	D	F	μ	K
3.8	10	0.155	0.42	3.8	10	0.117	0.35	3.8	10	0.086	0.07
3.8	20	0.138	0.06	3.8	20	0.108	-	3.8	20	0.079	0.60
3.8	30	0.165	-	3.8	30	0.103	-	3.8	30	0.078	0.85
25.0	10	0.137	5.28	25.0	10	0.036	0.24	25.0	10	0.059	0.27
25.0	20	0.122	1.05	25.0	20	0.061	0.72	25.0	20	0.029	0.46
25.0	30	0.121	0.01	25.0	30	0.059	3.44	25.0	30	0.035	1.09
38.0	10	0.100	20.78	38.0	10	0.047	0.30	38.0	10	0.230	2.35
38.0	20	0.106	32.86	38.0	20	0.039	0.21	38.0	20	0.023	14.08
38.0	30	0.090	21.15	38.0	30	0.046	0.09	38.0	30	0.073	0.06

** Midpoint condition $\mu_{avg} = 0.044$, standard deviation, $\sigma = 0.009$; $K_{avg} = 1.54$ $\sigma = 1.15$*

The other critical measurement taken was the frictional load on the load cell. The location of the load cell is at a one to one distance from the arm pivot. This corresponds to a one to one loading relationship between the load cell measurement and the radial loading of the arm relative to the rotating disk. The coefficient of friction is then approximated using the Equation 5-2:

$$\mu = \frac{F}{N} \tag{5-2}$$

where N is the dead weight load applied to the arm. The friction coefficient measurements were averaged over the duration of the low friction state and reported in Table 5-1 above. The nine repeats of the midpoint test condition and the control (midpoint condition with no lubricant) are plotted together in Figure 5-2.

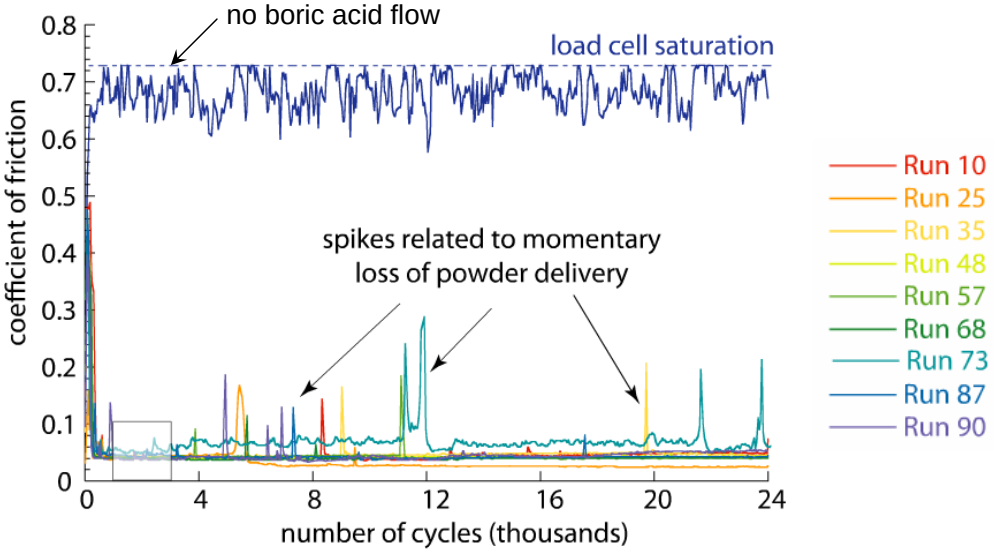

** Experimental conditions: Fn = 3.3 N, Ω = 2,000 RPM, D = 25.4 mm, f = 20 g/min.*

Figure 5-2. Friction coefficient versus cycle number for the 9 repeat tests and the control, which had no boric acid in the gas flow.

This plot displays the effect on friction coefficient of the boric acid as compared to interfacial contact with no lubricant. The figure shows how the boric acid, once introduced into

the contact interface, quickly reduced the friction coefficient. The spikes show interruptions in powder flow, and show the sensitivity of the system to the presence of the lubricant.

The powder delivery system experienced complete delivery failure on two experimental runs. This powder delivery failure occurred due to the delivery tubes clogging with powder. Figure 5-3 shows the effects of clogging on the friction coefficient.

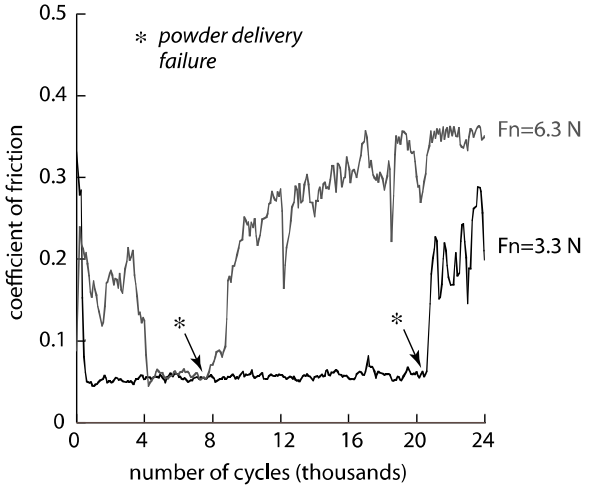

** Experimental conditions: D = 25 mm, surface speeds = 5.0 m/s, F_n identified in the plot.*

Figure 5-3. Friction coefficient versus cycle number for the experiments with terminal blockages in the boric acid delivery during the experiment.

The data was parsed several ways to search for trends in wear rate and friction coefficient. Since there were four variables in the experiment, a series of plots needed to be created. For each wear track diameter, three plots were created to detail the relationship between average friction coefficient and load, flow rate, and sliding speed, respectively. This series of plots is shown in Figures 5-4. Efforts were made to correlate the experimental data to the Von Karman mathematical model. Figure 5-5 shows the relationship between average friction coefficient and boundary layer thickness.

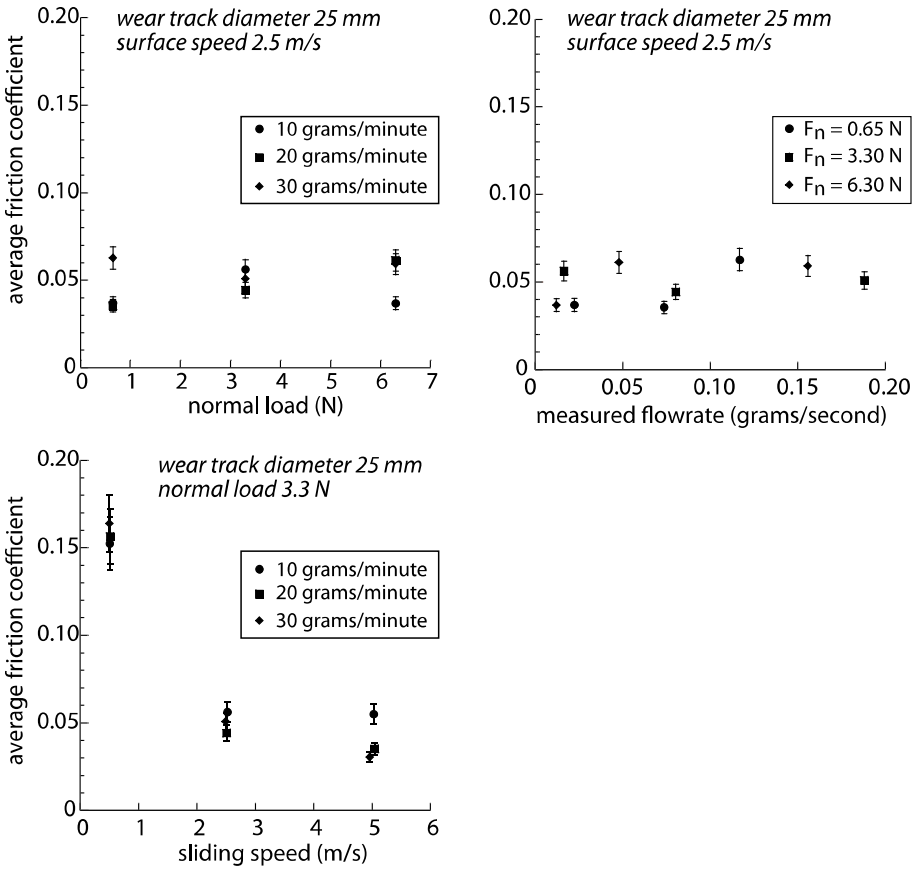

Figure 5-4. Average friction coefficient versus normal load, flow rate, and sliding speed.

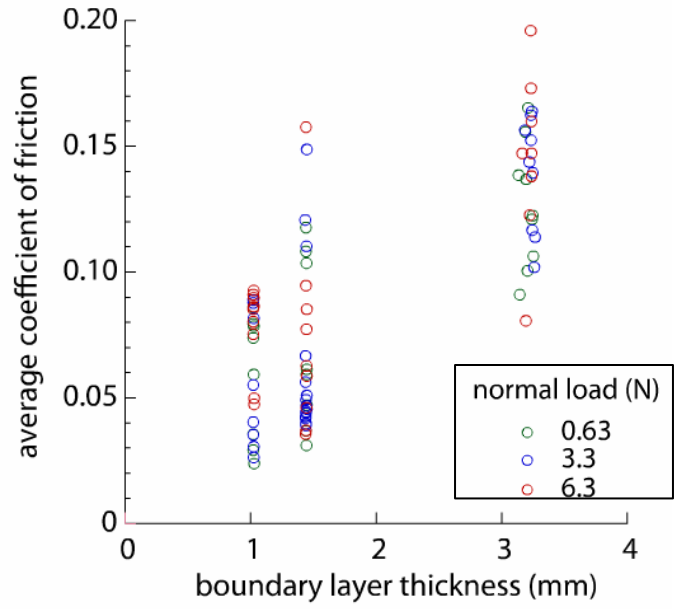

Figure 5-5. Average friction coefficients for all experiments plotted versus the boundary layer thickness. The data is separated for the various normal loads as indicated.

Many experiments showed a high degree of variability in the time taken to get to low friction. Though the exact reason for this variability was undetermined, it is hypothesized that unreliability in the powder delivery apparatus played a major role. As described in Chapter 4, many precautions were taken to ensure the powder would be clump free and the air would be properly desiccated. The mechanism responsible for delivering the boric acid powder to the Pin on Disk interface is unknown, but significant variability with the delivery was detected. Figure 5-6 shows two runs with different times to reach a low friction state. As is shown in the figure, the measured wear rates of the pin differ by two orders of magnitude. The measured friction coefficients are not significantly different.

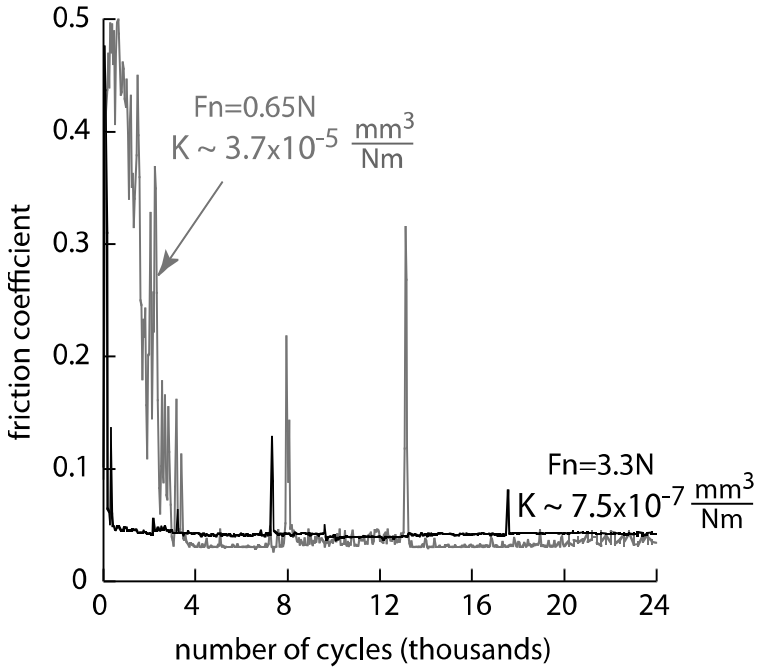

** Experimental Conditions: D = 25 mm, surface speed = 2.5 m/s, normal loads are identified in the figure.*

Figure 5-6. Friction coefficient versus cycle number for the two experiments that had the shortest and longest transients to low friction coefficient.

CHAPTER 6
DISCUSSION

When the boric acid was successfully flowing to the interface, friction and wear between the pin and disk was significantly reduced. This trend is shown in Figure 5-2, where the control condition is plotted against the midpoint runs. The only difference between the control and the midpoints runs was the presence of boric acid lubricant. The average friction coefficient drops from 0.641, non-lubricated sliding contact, to 9.3×10^{-4} when boric acid is introduced to the system. That represents a two order of magnitude reduction in friction force for the same operating conditions. The measured friction coefficient is rapidly impacted by the presence of boric acid in the contact interface. Figure 5-2 details how a low friction state is achieved after tens of revolutions.

The wear rate of the pin shows a similar trend to the friction reduction, reducing from 4.86 x 10^{-4} mm^3/Nm to 1.55 x 10^{-6} mm^3/Nm when boric acid is introduced into the sliding contact interface. Photographs detailing the difference in wear between the lubricated and non lubricated test conditions are shown in Figure 6-1.

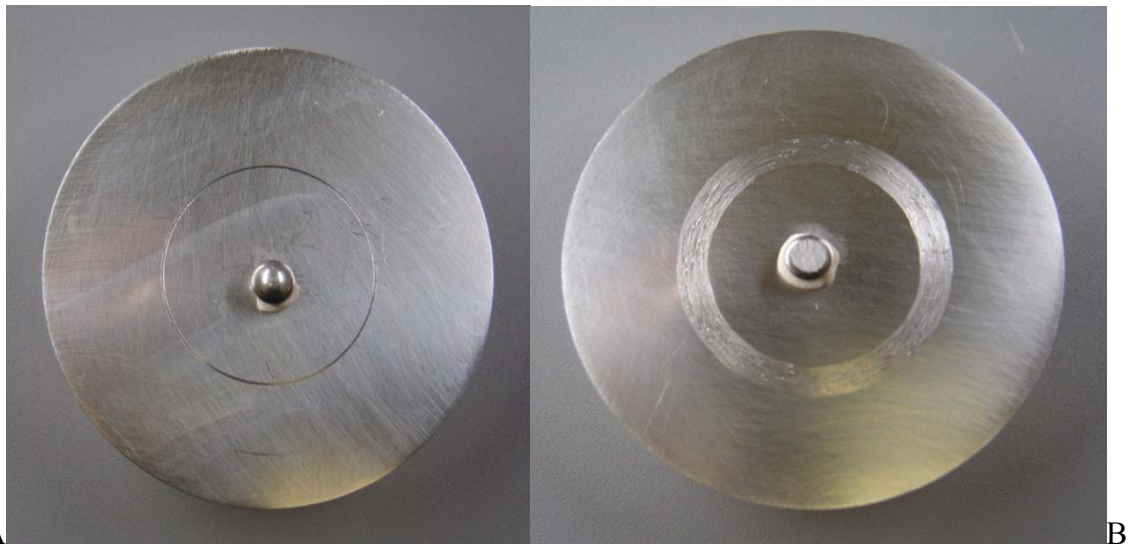

A B

Figure 6-1**.** Wear marks on pin and disk after midpoint experimental conditions A) with boric acid flow and B) without boric acid flow

The measured friction coefficient is very sensitivity to interruptions in flow. Figure 5-3 shows several spikes in friction coefficient that corresponded to perturbations in flow. In Figure 5-3, which highlights the two runs where the powder delivery system failed prematurely, the friction coefficient spikes at the point of failure and stays high for the duration of the run. As was seen with the intermittent delivery failures, the transition from low to high friction coefficient occurred within tens of revolutions. This transition from low to high friction suggests that the rate of powder deposition in the contact interface is very close to the rate of removal.

In Figure 5-4, the plots detail the effect on friction coefficient by a single experimental variable, while holding all other variables constant. Plot 5-4a show the effect of normal load on friction coefficient, in groups of powder flow rate, while holding wear track and surface speed constant. Across the data plots, there was no apparent significance between coefficient of friction and normal load or sliding speed. In Figure 5-4c, the lower sliding speeds resulted in a higher coefficient of friction than the higher sliding speed tests under the same conditions. Using the competitive rate models for the deposition and removal of boric acid, it is hypothesized that removal rate should increase with increasing sliding speed. This would lead to less boric acid getting entrained in the contact zone and result in a higher coefficient of friction. The experimental data suggested the opposite to be true. Several conclusions may be drawn from this data, however. It may suggest that the removal rate is suppressed at higher speed, thereby increasing the amount of boric acid in the interface and reducing friction. The data may also suggest that at higher sliding speeds, the rate of film formation on the surface of the disk and/or pin increases.

It is hypothesized that the direct injection of nitrogen and boric acid into the interface was not the primary mechanism for boric acid transport to the pin contact. Using the model solved

by Von Karman [13,14], it is hypothesized that the fluid flow generated across the rotation of the disk sample entrained the boric acid and delivered it to the pin contact. Figure 5-5 shows the results of Van Karman's flow model. The rotation of the spinning disk pulls air above the disk down at the center of the disk and discharges it radially outward. The air flow across the disk is assumed to be laminar if the Reynold's number is less than 300,000. The Reynold's number is given by Equation 6-1, where

$$\mathrm{Re} = \frac{V * R}{\nu} \tag{6-1}$$

Re is the Reynolds number (dimensionless), V is the peripheral speed (in m/s), R is the radius of the disk (in mm), and $\nu = 1.5x10^{-5}$ is used for the kinematic viscosity of the air. The highest Reynold's number encountered in this experiment was 4000, signifying that the flow across the disk was laminar. Rogers and Lance [24, 25] provided a numerical solution to this problem. Their study demonstrated that the boundary layer thickness, δ, is relatively constant across the disk and varies inversely with the square-root of the angular speed. The following equation describes the results of their study

$$\delta = 5.4\sqrt{\frac{\nu}{\omega}} \tag{6-2}$$

where ω is the angular speed of the disk (in rad/s), and again $\nu = 1.5x10^{-5}$ m^2/s is used for the kinematic viscosity of air. The entire data set is plotted versus the calculated boundary layer thickness in Figure 5-5. The data trends in Figure 5-5 suggest that the thinner and higher speed flows are more efficient at delivering boric acid to the contact.

Figure 5-2 details the measured friction coefficient for unlubricated pin on disk stainless steel contact. The average wear rate was measured to be $K = 5.0x10^{-4}$ mm^3/Nm. All lubricated experiments conducted showed significant decreases in pin wear rate, as shown in Table 5-1.

Eleven of the pin samples showed no detectable wear marks, these are indicated by dashes in the wear rate column of Table 5-1. The lowest measured wear rate was $K = 7.5 \times 10^{-4}$ mm^3/Nm, which occurred during the 25 mm diameter, 3.3 N load, 2.5 m/s sliding speed, and 0.078 grams/second boric acid flowrate conditions. The experiments exhibit over 500 times greater improvement in wear resistance over the unlubricated contact measurements.

Substantial effort was made to correlate the friction coefficient and the wear rate with the selected experimental variables. There were no strong indicators tying the experimental variables to either friction coefficient or wear rate. The only qualitative explanation for the variation in wear rate is the significant loss of material during start up transients. The tests were initiated on nascent surfaces with the boric acid flow expected create to replenish a surface film *in situ*. The startup transient varied widely between experimental runs, though all experiments eventually reached a low friction state. It is suggested that the majority of material lost to wear occurs during this period, and better understanding of the film formation must be developed. Figure 5-6 shows the friction coefficient plots for experiments with the shortest and longest initial transient conditions.

These experiments were both at a radial position of 2.5 mm and a sliding speed of 2.5 m/s, although they were at two different normal loads. The experiment with the shortest transient had a wear-rate of 7.5×10^{-7} mm^3/(Nm) and the test with the longest transient had a wear-rate of 3.7×10^{-5} mm^3/(Nm). The ratio of the volumes lost between the shortest and longest transient was 0.1 (i.e., the test with a shorter transient lost 10 percent of the material of the test with the longest transient), while the ratio of the frictional energy dissipated during the transient region is about 1/3.

CHAPTER 7
CONCLUSIONS

- **Conclusion 1:** These experiments were the first reported demonstrations of continuous powder delivery of boric acid as a solid lubricant.

- **Conclusion 2**: These experiments clearly indicate that powder delivery of boric acid is a viable technique for providing *in situ* lubrication for concentrated metal contacts. Wear rate reductions of over 100 times and friction coefficients of well under 0.1 were demonstrated.

- **Conclusion 3**: Further development and refinement of the powder delivery system must be explored to develop an accurate understanding of the impact of the variables on friction coefficient and wear rate.

- **Conclusion 4**: A future study is suggested for exploring the impact of a pre-deposited boric acid film on the surface of pin and/or disk to verify the impact of the initial transient on friction coefficient and wear rate.

LIST OF REFERENCES

[1] P. Hamblin, Environmentally compatible lubricants: trends, standards, and terms. Proc. Environmental Aspects in Production and Utilization of Lubricants, Sopron, (1995) 1-10

[2] W. Bartz, Lubricants and the environment, Tribology International 31 (1998) 35-47

[3] G. Johnson, Milacron Marketing Co, CIMCOOL technical report, (1999) 1-12

[4] A.R. Machado, J. Wallbank, The effect of extremely low lubricant volumes in machining, Wear 210 (1997) 76-82

[5] M. Rahman, A. Senthil-Kumar, Salam M.U., Experimental evaluation on the effect of minimal quantities of lubricant in milling, International Journal of Maching Tools and Manufacture 42 (2002) 539-547

[6] F.M. Kustas, L. FehrehnbacheR, R. Komanduri, Nanocoatings in cutting tools for dry machining, Annals of the CIRP (1997) 39-42

[7] L.W. Jelinski, T. Graedel, R. Laudise, D.W. McCall, C.K Patel, Industrial ecology: concepts and approaches, Proceedings of the National Academy of Sciences of the United States of America 89 (1992) 793-797

[8] L. Ward, Influence of boric acid and borax on digestion and health, Science 20 (1904) 26-27

[9] G. Brown Jr, Remarks on industrial ecology, Proceedings from the National Academy of Sciences 89 (1992) 876-878

[10] J. Sutherland, K. Gunter, D. Allen, D. Bauer, B. Bras, T. Gutowski, C. Murphy, T. Piwonka, P. Sheng, D. Thurston, E. Wolff, A global perspective on the environmental challenges facing the automotive industry: State-of-the-art and directions for the future, Int J Vehicle Des 35 (2004) 86-110.

[11] D. Allen, D. Bauer, B. Bras, T. Gutowski, C. Murphy, T. Piwonka, P. Sheng, J. Sutherland, D. Thurston, E. Wolff, Environmentally benign manufacturing: Trends in Europe, Japan, and the Usa, J Manuf Scie E-T ASME 124 (2002) 908-920.

[12] P. Lyday, Mineral commodity summaries, US Geological Survey, (2003) 110-122.

[13] A. Erdemir, Tribological properties of boric-acid and boric-acid-forming surfaces.1. Crystal-chemistry and mechanism of self-lubrication of boric-acid, Lubr Eng 47 (1991) 168-173.

[14] A. Erdemir, R. Erck, and J. Robles, Relationship of hertzian contact pressure to friction behavior of self-lubricating boric-acid films, Surf Coat Tech 49 (1991) 435-438.

[15] A. Erdemir, G. Fenske, and R. Erck, A study of the formation and self-lubrication mechanisms of boric-acid films on boric oxide coatings, Surf Coat Tech 43-4 (1990) 588-596.

[16] A. Erdemir, G. Fenske, R. Erck, F. Nichols, D. Busch, Tribological properties of boric-acid and boric-acid-forming surfaces. 2. Mechanisms of formation and self-lubrication of boric-acid films on boron-containing and boric oxide-containing surfaces, Lubr Eng 47 (1991) 179-184.

[17] B. Gearing, H. Moon, and L. Anand, A plasticity model for interface friction: Application to sheet metal forming, International Journal of Plasticity 17 (2001) 237-271.

[18] I. Singer, R. Bolster, J. Wegand, S. Fayeulle, B. Stupp, Hertzian stress contribution to low friction behavior of thin mos2 coatings, Appl Phys Lett 57 (1990) 995-997.

[19] M. Lovell, W.G. Sawyer, and A. Mobley, On the friction and wear performance of boric acid lubricant combinations in extended duration processes, Tribol Tech 25 (2005) 73-81.

[20] N. Mccook, D. Burris, G. Bourne, J. Steffens, J. Hanrahan, W.G. Sawyer, Wear resistant solid lubricant coating made from ptfe and epoxy, Tribo Lett 18 (2005) 119-124.

[21] T. Von Karman, Uber laminare und turbulente reibung, Z Angew Math Phys 1 (1921) 233-252.

[22] M. Miklavcic, C. Wang, The flow due to a rough rotating disk, Z Angew Math Phys 55 (2004) 235-246.

[23] M. Rogers, G. Lance, The rotationally symmetric flow of a viscous fluid in the presence of an infinite rotating disk, J Fluid Mech 7 (1960) 617-631.

[24] M. Rogers, G. Lance, Boundary layer on disc of finite radius in rotating fluid, Q J Mech Appl Math 17 (1964) 319-25.

BIOGRAPHICAL SKETCH

The author was born in Oakland, California, in 1977. Timothy Barton was raised in the San Francisco bay area for the duration of his childhood. In 1995, he moved to Florida to attend the University of Florida to pursue a degree in mechanical engineering. He graduated with his Bachelor of Science in mechanical and aerospace engineering in 2001. He obtained his Master of Science in mechanical and aerospace engineering from the University of Florida in 2007.